

SEPARATION OF PRIMARY AMORPHOUS SILICATES AND CAPTURE-RELATED GLASSES IN STARDUST COMETARY SAMPLES. C. H. van der Bogert¹, T. Stephan², and E. K. Jessberger¹, ¹Institut für Planetologie, Westfälische Wilhelms-Universität Münster, 48149 Münster, Germany (vanderbogert@uni-muenster.de), ²Department of Geophysical Sciences, University of Chicago, Chicago, IL 60637, USA.

Introduction: Based on astronomical observations and astrophysical models, comets have traditionally been thought to be assembled from amorphous silicate dust with both solar and interstellar origin. In addition, amorphous silicates are present in IDPs [e.g., 1] and primitive meteorite matrices [e.g., 2], albeit not as a dominant phase. These observations require a mechanism for the transformation of amorphous silicates in nebular clouds into the crystalline materials seen in primitive planetary materials, including IDPs and primitive meteorites [3].

Initial analyses of Stardust cometary particles have shown that 81P/Wild 2 is composed of an unequilibrated mixture of crystalline phases exhibiting a surprising range of formation conditions [4,5]. This requires that minerals from a wide cross-section of the protosolar nebula were mixed into the region of space where 81P/Wild 2 formed [4,5]. In addition, only a few grains with interstellar origins have been found—many fewer than expected [e.g., 6,7].

So far, these results are at odds with the aforementioned comet formation models. However, in order to fully test these models with Stardust samples, a thorough understanding of the capture-processing of the samples is necessary, because of the destruction of fragile cometary materials and the formation of secondary amorphous phases unrelated to potential primary amorphous silicates. In addition to the capture-related melting of the cometary particles, the search for primary amorphous silicates is complicated by the presence of the aerogel capture medium (amorphous SiO₂), capture-melted and compressed aerogel, and mixtures of these aerogel products with melted cometary materials [e.g., 8,9,10]. Our approach is to study both capture-melted and unmelted materials to first characterize the effects of capture-processing on the cometary particles. Then, it may be possible to separate capture-processed materials from preexisting amorphous phases.

Methods: The samples were first analyzed using time-of-flight secondary ion mass spectrometry (TOF-SIMS) [11,12]. These data provided compositional overviews of the grains, which were used to pinpoint areas of interest for transmission electron microscopy (TEM).

Samples: The samples included materials from the edges of impact tracks and terminal particles (Fig. 1), representing both capture-melted and relatively pristine cometary material.

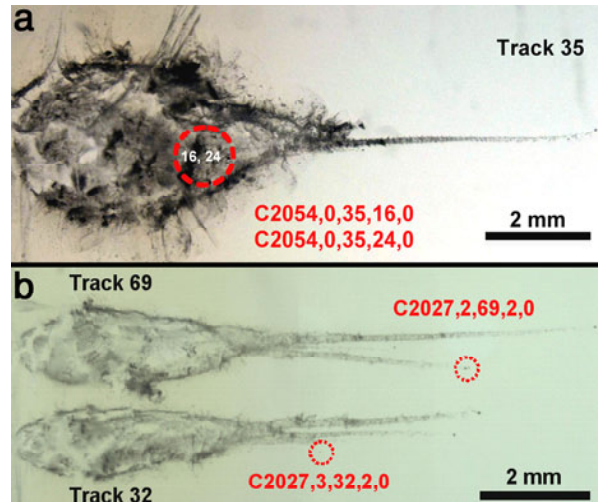


Figure 1. (a) Stardust cometary aerogel cell C2054, impact track 35. The investigated particles (TEM grids C2054,0,35,16,9 and C2054,0,35,24,5) are both from the margin of the bulbous entry cavity. (b) Stardust cometary aerogel cell C2027, impact tracks 32 and 69. The investigated particles (TEM grids C2027,3,32,2,6 and C2027,2,69,2,5) are both terminal particles.

Capture-melted particles. Samples extracted from the walls of the bulbous cavities are frequently mixed composition glasses that likely represent cometary material melted and mixed with melted and compressed aerogel during the capture process [8,13]. These materials serve as examples of capture-melted materials for comparison with possible primary amorphous cometary silicates. TEM grids C2054,0,35,16,9 #44 and C2054,0,35,24,5 #19 are both composed mainly of silica-rich glass with varying concentrations of Fe, Mg, and Si as determined by both TOF-SIMS and TEM EDX analyses [8,14]. These glasses contain finely dispersed FeNi and FeS spherules, which melted during the capture process and recrystallized (Fig 2a).

Terminal particles. The cometary particles least affected by their impact into the aerogel capture medium were those particles that survived the initial impact and traveled deepest into the aerogel, i.e., “terminal particles”. These particles were likely larger and more coherent, thus more resistant to impact processing [e.g., 13]. It is in these particles where the successful identification of primary amorphous silicates is most likely.

Two terminal particles were analyzed for this study: C2027,3,32,2,6 #20 and C2027,2,69,2,5 #25. Both particles exhibited a thin external coating of

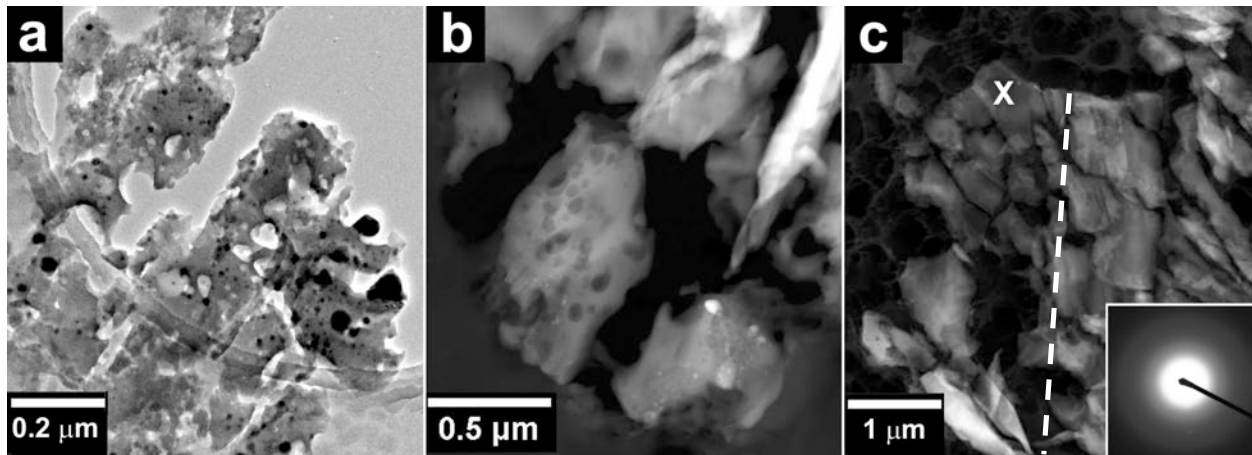


Figure 2. (a) Bright field TEM image from C2054,0,35,24,5 #19, showing the typical texture for the capture-melted samples in our study—frothy, melted aerogel with dispersed FeNi and FeS spherules. (b) HAADF TEM image of material similar to that in (a), adhered to terminal particle C2027,3,32,2,6 #20. (c) HAADF TEM image of anorthitic area (left of the dashed line) in sample C2027,2,69,2,5 #25, with an example of an amorphous diffraction pattern from spot 'X'. This material did not contain dispersed metallic phases or vesicles.

compressed and melted aerogel. The margins of particle C2027,3,32,2,6 #20 exhibit small areas of glassy material with finely dispersed, submicron metallic blebs (Fig. 2b), similar to the capture-melted material in Fig. 2a. Both samples, however, are composed primarily of large mineral grains, in stark contrast to the capture-melted particles. TOF-SIMS analyses suggest the presence of pyroxene and a Ca,Al-rich phase, possibly anorthite in sample C2027,2,69,2,5 #25 [12]. When investigated using TEM, the anorthitic area exhibited both crystalline and amorphous diffraction patterns (Fig 2c). This area does not contain dispersed FeNi and FeS blebs or vesicles that were seen in capture-melted materials shown in Figs. 2a,b. TEM EDX analyses also confirm that this area is anorthitic in composition.

Discussion: The detection of primary amorphous silicates in Stardust cometary samples is clearly important for their comparison with IDPs, primitive meteorites, astronomical observations, and astrophysical models. However, there are several factors that make it difficult to unequivocally identify primary amorphous silicates in the Stardust samples. The most significant challenge is their separation from melted and compressed aerogel. For example, this confounds the identification of possible GEMS in Stardust samples [10]. Unfortunately, there is no tracer in the aerogel that can unequivocally identify its presence or absence.

However, we think it is likely that the amorphous material in C2027,2,69,2,5 #25 is not melted aerogel, because it has an anorthitic composition, rather than a non-stoichiometric composition with excess Si, and it does not contain the dispersed FeNi and FeS spherules

or vesicles seen in the capture-melted (Fig. 2a) and adhered materials (Fig. 2b). Alternately, it is possible that exposure to the TEM electron beam caused the transformation of crystalline anorthite to amorphous material despite our efforts to limit beam exposure. However, there were no obvious signs of beam damage, such as developing spottiness, seen in other types of feldspars during TEM analyses [e.g., 15]. In conclusion, we think that the amorphous anorthite may be primary amorphous silicate glass from 81P/Wild 2.

Other primary amorphous silicates, including amorphous olivine and pyroxene, may also be present in Stardust cometary samples. Further characterization of capture-melted materials will help to separate capture-melted materials from primary amorphous silicates, the presence or absence of which constrain models of comet formation and evolution.

References: [1] Hanner and Bradley (2004) In *Comets II*, 555-564. [2] Scott (2007) *Ann. Rev. Earth Planet. Sci.* 35, 577-620. [3] Nuth, et al. (2002) *MAPS* 37, 1579-1590. [4] Zolensky, et al. (2006) *Science* 314, 1735-1739. [5] Brownlee, et al. (2006) *Science* 314, 1711-1716. [6] McKeegan, et al. (2006) *Science* 314, 1724-1728. [7] Stadermann, et al. (2008) *MAPS* 43, 299-313. [8] van der Bogert and Stephan (2008) *LPS* 39, #1732. [9] Leroux, et al. (2008) *MAPS* 43, 97-120. [10] Ishii, et al. (2008) *Science* 319, 447-450. [11] Stephan and van der Bogert (2008) *LPS* 39, #1508. [12] Stephan (2008) *MAPS* 43, 233-246. [13] van der Bogert, et al. (2008) *EPSC* 3, #546. [14] Stephan, et al. (2008) *MAPS* 43, 285-298. [15] Hellmann, et al. (2003) *Phys. Chem. Min.* 30, 192-197.

Acknowledgements: This work was supported through Deutsche Forschungsgemeinschaft grant #STE576/17-2, NASA grant #NNX07AL94G, and the Oxford University/EU-ESTEEM program contract #026019.